

西南日本の沈み込み帯メランジュ中のヒスイ輝石岩に記録された塩水 Saline fluids recorded in jadeitites in subduction-zone melanges of southwest Japan

森 康^{1*}; 重野 未来¹; 川本 竜彦²; 西山 忠男³

MORI, Yasushi^{1*}; SHIGENO, Miki¹; KAWAMOTO, Tatsuhiko²; NISHIYAMA, Tadao³

¹北九州市立自然史・歴史博物館, ²京都大学地球熱学研究施設, ³熊本大学自然科学研究科

¹Kitakyushu Mus. Nat. Hist. Hum. Hist., ²Inst. Geotherm. Sci., Kyoto Univ., ³Grad. Sch. Sci. Tech., Kumamoto Univ.

Slab-derived fluids play essential roles in mass transfer along subduction-zone channels between the subducting slab and mantle wedge (e.g., Bebout 2013 Metasomatism and the chemical transformation of rocks; Spandler and Pirard 2013 Lithos). Salinity of such slab-fluids probably affects solubility and fluid-rock partitioning of elements; therefore, it remains to be investigated in various rocks. Jadeitite is a rock composed mainly of jadeite (sodium pyroxene, NaAlSi₂O₆) and occurs typically in serpentinite mélanges intercalated to high-pressure and low-temperature metamorphic belts. This curious rock is thought to be the product of direct precipitation from aqueous fluids and/or of fluid-induced metasomatism of a protolith (Harlow *et al.* 2007 Geology of gem deposits, Tsujimori and Harlow 2012 Eur J Mineral, and references therein). Fluid inclusions are commonly observed in jadeitites, and they may provide information about the fluid composition in subduction-zone mélanges. We determined major components and salinity of fluid inclusions in the jadeitites collected from eight localities in Japan: Omi-Itoigawa (Omi-Renge belt), Oya and Osa (Suo belt), Kochi (Kurosegawa belt), Mie and Tone (Nishisonogi metamorphic rocks), and Shimonita and Yorii (the origin unclear). In all of the studied rocks, primary fluid inclusions consist of a liquid phase and a gas bubble. Raman spectra show the presence of H₂O liquid and vapor with or without minor CH₄ gas. The freezing point of the liquid phase indicates high-salinity (up to 8 wt% NaCl equivalent) of the primary fluid inclusions. The salinity varies among the localities of the jadeitite. For example, the salinity of the primary fluid inclusions is about 7.1 ± 0.1 wt% NaCl equivalent in the albite jadeitite from Oya and about 4.6 ± 1.2 wt% NaCl equivalent in quartz inclusions bearing jadeitite from Tone. Some jadeitite samples contain secondary CH₄-rich fluid inclusions along healed microcracks. The presence of minor CH₄ is also reported in the saline fluids inclusions with 5.1 ± 1.9 wt% NaCl equivalent from the Myanmar jadeitite (Shi *et al.*, 2005 Geochem J). The present findings suggest that saline fluids with or without CH₄ are common in subduction-zone mélanges in Japan as well as in Myanmar. The reduced conditions can be caused by serpentinitization processes. This is contrast to the CO₂-bearing saline fluids in the peridotite xenoliths from fore-arc mantle wedge (Kawamoto *et al.*, 2013 PNAS). The high-salinity of the slab-fluids probably enhances the mobility of elements such as Pb in subduction-zone channels (Keppler, 1996 Nature, Shigeno *et al.*, 2012 Eur J Mineral).

キーワード: 塩水, ヒスイ輝石岩, 流体包有物, 蛇紋岩メランジュ, 沈み込み帯

Keywords: saline fluid, jadeitite, fluid inclusion, serpentinite mélange, subduction zone

沈み込み境界上盤の蛇紋岩構造：三波川帯の天然の例 Serpentinite structure above subduction surface: Analysis of a natural example in Sanbagawa metamorphic belt

水上 知行^{1*}; 曾田 祐介¹; 横山 寛紀¹; 平松 良浩¹

MIZUKAMI, Tomoyuki^{1*}; SODA, Yusuke¹; YOKOYAMA, Hironori¹; HIRAMATSU, Yoshihiro¹

¹ 金沢大学

¹ Kanazawa University

Serpentinization is a key reaction in forearc mantle. Formation of strong schistosity and shear zones under high differential stresses provides anastomosing networks of fluid pathways as well as seismically anisotropic nature in the mantle. Understanding of such structural development is important for both interpretation of seismic analyses and forward modelling of subduction system including thermal structure, material circulation, magma process and slip behaviours of subduction boundaries.

We report results of petrological and structural analyses of layered antigorite (Atg) serpentinite in the marginal part of the Higashi-akaishi ultramafic unit in the Sanbagawa belt. This is a product of hydration of dunite (a rock consisting of almost 100% olivine (Ol)) due to metamorphic fluid from the underlying meta-sediments and meta-basites. Strong shape preferred orientation of Atg and existence of boudinaged layers indicate fluid-rock reaction under extensional deformation.

The layered structure is defined by a centimeter to meter-scale interlayering between Ol-rich and Atg-rich units. The modal amounts of Atg in these units form peaks at 15 vol% and 50 vol%, respectively, showing a bi-modal distribution as a whole. Effects of initial microstructures on the extent of serpentinization are limited: Porphyroclastic and fine-grained dunite, that occupy a large part of the outcrop, are transformed to both Ol-rich and Atg-rich layers although dunite with more than 50% of coarse Ol grains has been poorly serpentinized. Each Atg layer shows millimeter-scale spaced foliations defined by amounts of Ol and Atg and locally shows a diffusive variation in millimeter to centimeter-scales. Thickness and proportion of Atg-rich layers increase near the contact with crustal rocks.

Reaction for the Atg formation is constrained based on re-distribution of elements among Ol, Atg and opaque minerals. As serpentinization proceeds, Ol is enriched in Fe and Ni owing to their incompatibility in Atg. Taking concomitant formations of minor amounts of magnetite and sulfides into account, the variation of the Ol composition and modal amounts of serpentinization products are quantitatively explained by the following reaction: $Ol + SiO_{2,aq} + H_2O \Rightarrow Atg$. This indicates that the development of Atg has been controlled by a supply of silica in aqueous fluids.

We measured thickness of 70 layers for each and, taking the layers with the thickness lower than 200 centimeters, we found exponential relationships in cumulative frequency distributions both for Ol-rich and Atg-rich layers. Relative thickness between neighbouring units $[d(Ol)/d(Atg)]$ also shows an exponential distribution. We could not find any regular relationships among width and spacing like Liesegang patterns.

It is known that pattern structures appear in reaction-diffusion systems. The above observations strongly suggest that the development of layered structures in Atg serpentinite is controlled by interaction between reaction and material transfer. In this case, potential causes of heterogeneous serpentinization may be diffusional contrast between H_2O and SiO_2 or permeability contrast between Ol-rich and Atg-rich layers. Scaling analyses of deep low frequency tremors showed that duration-amplitude and size-frequency distributions of tremors in SW Japan can be fit with exponential models rather than power-law models. The seismological observations imply structural heterogeneity with unique scale length. Further examination on the exponential relationships developed in serpentinite may contribute to understand the slip phenomena on plate interfaces.

Keywords: serpentinite, layered structure, reaction-diffusion, exponential frequency distribution, deep low frequency tremor

福島県大島半島に産する蛇紋岩中のアワルワ鉱 Awaruite in serpentinites from Oshima Peninsula, Fukui Prefecture, Japan

山口 海^{1*}; 上原 誠一郎²
YAMAGUCHI, Kai^{1*}; UEHARA, Seiichiro²

¹九州大学大学院理学府地球惑星科学専攻, ²九州大学大学院理学研究院地球惑星科学部門

¹Department of Earth and Planetary Sciences, Faculty of Science, Kyushu University, ²Department of Earth and Planetary Sciences, Faculty of Science, Kyushu University

Awaruite is one of native Ni-Fe alloys, and the compositional range is Ni₂Fe to Ni₃Fe. The space group is *Fm3m* or *Pm3m* (e.g., Williams, 1960; Ahmed et al., 1981). Typical grain sizes are 10-300 μm, and grain shapes are typically irregular, anhedral or skeletal. It is found only in the serpentinized peridotites and chondritic meteorites (e.g., Ramdohr, 1967; Clarke et al., 1970). In general, awaruite is observed in serpentine vein (Sakai and Kuroda, 1983), and coexist with other metal minerals (Kanehira et al., 1975). This study deals with the characteristic occurrence of awaruite in pseudomorph texture in the Oshima serpentinites from Oshima peninsula, Fukui prefecture, Japan.

All samples were examined with polarizing microscope observation, X-ray diffraction analysis and SEM-EDS analyses. Preparation of TEM specimen and microtexture observation were conducted with an ion milling machine (JEOL EM-09100IS) and TEM (JEOL JEM-2000FX, JEM-3200FSK) in the Research Laboratory for High Voltage Electron Microscopy (HVEM), Kyushu University, Japan. Chemical analyses of microtexture were also examined using JEM-3200FSK equipped with EDS.

Peridotites in this area are partially or perfectly serpentinized. Texture of the serpentinite is mesh texture after forsterite and vein texture. Scarcely serpentinized enstatite is also observed. Each mesh texture is composed of mesh rim shows optical anisotropy and mesh core shows optical isotropy. The serpentinization of mesh texture is strong in close to vein textures. Most mesh rims near vein texture consist of some layers; outer rim, outer-inner rim boundary and inner rim. These rims consist of chrysotile, about 50 nm in width and 2 μm in length, and lizardite, about 300 nm in width and 1 μm in length, and outer-inner rim boundary about 2 μm in width are filled with serpentine fine grains, up to 100 nm in diameter.

A number of awaruite fine grains, 200-300 nm diameter, array along cell boundary, outer-inner rim boundary and rim-core boundary. These awaruite coexist with no other metal minerals; pentlandite, magnetite and etc. In contrast, metal minerals in vein texture are magnetite and minor pentlandite. These results indicate that mesh texture in serpentinite is extremely reductive environment compared with vein texture. The chemical composition of awaruite (average of four analysis) is Ni 73.13% and Fe 26.87%. The cross-section of these awaruite grains is square or rhombic, indicating that these grains are cube or octahedral crystals (fig. 1a). These grains seem to be euhedral from grain shapes, and this is characteristic compared with previous studies (e.g., Rubin, 1991). The SAED pattern recorded along the [001] zone axis shows strong 200, 220 reflections and weak 100, 110 reflections (fig. 1b). This indicates space group of the Oshima awaruite is *Pm3m*, which is ordering phase of *Fm3m* awaruite. Lower symmetry of the Oshima awaruite will be formed lower temperature.

キーワード: アワルワ鉱, 網目状組織, 蛇紋岩, 微細組織, 蛇紋石鉱物, 透過電子顕微鏡

Keywords: Awaruite, Mesh texture, Serpentinite, Microtexture, Serpentine minerals, TEM

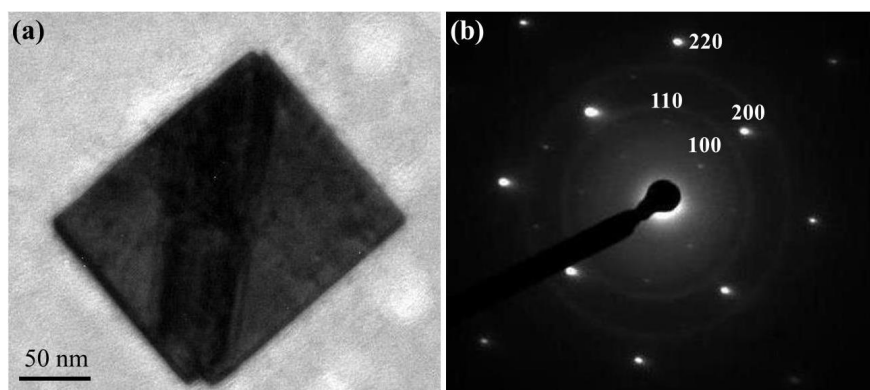


Fig. 1. (a) TEM image of awaruite in mesh texture. (b) The SAED pattern of (a) recorded along the [100] zone axis.

アンチゴライト CPO の測定 Antigorite CPO measured by U-stage, EBSD and synchrotron X-rays

曾田 祐介^{1*}; 安東 淳一²; 浦田 義人²; Wenk Hans-Rudolf³
SODA, Yusuke^{1*}; ANDO, Jun-ichi²; URATA, Yoshito²; WENK, Hans-rudolf³

¹ 金沢大学, ² 広島大学, ³ カリフォルニア州立大学

¹Kanazawa University, ²Hiroshima University, ³University of California, Berkeley

Foliated antigorite serpentinite with crystallographic preferred orientation (CPO) probably causes shear wave splitting observed at subduction zones (e.g., Katayama et al., 2009). Therefore, the study of type and intensity of antigorite CPO is an important to understand the detail of this phenomenon.

Soda and Wenk (2014) measured CPOs of antigorite serpentinite from the Sashu Fault at the Saganoseki Peninsula, Oita Prefecture, by three independent methods, U-stage (with optic microscope), EBSD and synchrotron X-rays. The obtained antigorite CPOs by three methods are almost same without the fabric strength, maxima of pole figures in multiples of random distribution. The fabric strength decreases in the following order, U-stage >EBSD >synchrotron X-rays, which is probably caused by the characteristics of three methods. Through U-stage measurement, we can obtain the fabric pattern of antigorite CPO mainly from coarser antigorite grains (>30 μm). In the case of EBSD measurement, we measure antigorite CPO within an area of ca. 0.8 mm \times 0.8 mm. Measurement points of only ca. 30% can be used to make fabric patterns. Residual ca. 70% points are neglect, because the quality of Kikuchi lines from them is too low to identify the orientation. In the synchrotron X-rays method, the result represents the bulk fabric from a volume of ca. 0.5 mm \times 0.5 mm \times 1.0mm.

The serpentinite measured antigorite CPO develops mylonitic structures with a penetrative foliation and lineation (Soda and Takagi, 2010). The antigorite grains show undulose extinction. And their grain boundary is unclear under the microscopy. Mg# (Mg/(Mg+Fe)) of antigorite grains is wide range 0.98-0.88. The BSE images indicate Fe-rich antigorite infilling the grain boundaries and fractures of Mg-rich antigorite.

The same serpentinite has already observed by TEM (Urata et al., 2009). The results indicate that the m-values of antigorite grains, the number of octahedral along the [100] modulation wave, make two groups, high m-value (16-18) and low m-value (13-14). This result suggests that the antigorite are crystallized mainly two stages, which is supported by the variation of Fe contents of antigorite (Fe-rich and Mg-rich). The Mg-rich antigorite grains are main minerals composed of the serpentinite, Fe-rich antigorite grains occupy at the periphery of the others and within the vein. The TEM observation indicates that the Mg-rich antigorite grains are subdivided into sub-grain with 50-100 nm in size, which can be recognized as an undulose extinction under optic microscope.

These microstructures of antigorite grains potentially influence the outcome of CPO measurements. The weaker fabric patterns from the synchrotron X-rays are probably attributed to the fine-grained antigorite crystallized at the deferent stages and to sub-grain. And the U-stage and EBSD measurements focus only the selected grains, which may result in overestimation of elastic wave anisotropy of serpentinite.

References

- Katayama et al, 2009, Nature 461, 1114-1117.
- Soda and Takagi, 2010, Journal of Structural Geology 32, 792-802.
- Soda and Wenk, 2014, Tectonophysics, in press
- Urata et al., 2009, AGU2009 abstract. MR41A-1858.

キーワード: アンチゴライト, CPO, シンクロトロン X 線, 弾性波異方性
Keywords: antigorite, CPO, synchrotron X-ray, elastic anisotropy

Olivine CPO in non-deformed peridotite due to topotactic replacement of antigorite Olivine CPO in non-deformed peridotite due to topotactic replacement of antigorite

永治 方敬¹; ウォリス サイモン^{1*}; 小林 広明¹; 道林 克禎²; 水上 知行³; 瀬戸 雄介⁴; 三宅 亮⁵; 松本 恵⁶
NAGAYA, Takayoshi¹; WALLIS, Simon^{1*}; KOBAYASHI, Hiroaki¹; MICHIBAYASHI, Katsuyoshi²; MIZUKAMI, Tomoyuki³
; SETO, Yusuke⁴; MIYAKE, Akira⁵; MATSUMOTO, Megumi⁶

¹Department of Earth and Planetary Sciences, Nagoya Nagoya University, ²Institute of Geosciences, Shizuoka University, ³Department of Earth Science, Kanazawa University, ⁴Department of Earth and Planetary Science, Kobe University, ⁵Department of Earth and Planetary Science, Kyoto University, ⁶Center for Supports to Research and Education Activities, Kobe University
¹Department of Earth and Planetary Sciences, Nagoya Nagoya University, ²Institute of Geosciences, Shizuoka University, ³Department of Earth Science, Kanazawa University, ⁴Department of Earth and Planetary Science, Kobe University, ⁵Department of Earth and Planetary Science, Kyoto University, ⁶Center for Supports to Research and Education Activities, Kobe University

Olivine crystallographic preferred orientation (CPO) is thought to be the main cause of seismic anisotropy in the mantle, and its formation is generally considered to be the result of plastic deformation of mantle by dislocation creep. Olivine CPO has been reproduced in laboratory deformation experiments and considerable success has been achieved in understanding the deformation conditions (e.g. stress, temperature and water content) under which different olivine CPO patterns develop. This opens the possibility of mapping conditions in the mantle using seismic anisotropy and has been the subject of considerable study. Here we report an alternative mechanism for olivine CPO without the need for deformation. This process may be important in understanding the seismic properties of mantle in convergent margins.

Metamorphic studies show peridotite in the Happo area, central Japan, formed by the dehydration of antigorite-schist related to contact metamorphism around a granite intrusion. Both field and microstructural observations suggest the olivine has not undergone strong plastic deformation. This was confirmed by TEM work that shows the olivine has very low dislocation densities and lacks low angle tilt boundaries. Such tilt boundaries are general stable even after annealing. These features show that peridotite in the Happo area formed in the absence of solid-state deformation.

The olivine of the Happo peridotite formed dominantly by the dehydration breakdown of antigorite schist. We propose that the olivine CPO formed as a result of topotactic replacement of antigorite by the newly formed olivine. EBSD measurements in samples where both antigorite and new olivine are present and in contact show a very close crystallographic relationship between the two minerals: the *a*-axes are parallel, and the *b*- and *c*-axes are perpendicular. We conclude the strong olivine CPO in the Happo area was inherited from the original CPO of the antigorite. Such a process is likely to also occur in subduction zones where serpentinite is dragged down by plate movement. Topotactic growth of olivine may be an important cause of mantle anisotropy in convergent margins.

キーワード: subduction zones, microstructure, B-type olivine CPO, antigorite, topotaxy
Keywords: subduction zones, microstructure, B-type olivine CPO, antigorite, topotaxy

Cr-rich olivine in deserpentinized peridotite and its implication Cr-rich olivine in deserpentinized peridotite and its implication

遠藤 俊祐^{1*}

ENDO, Shunsuke^{1*}

¹産総研 地質情報

¹Institute of Geology and Geoinformation, AIST

Formation of Cr-rich olivine ($\text{Cr}_2\text{O}_3 > 0.1 \text{ wt } \%$) in the presence of Cr-spinel \pm pyroxene has been thought to require extremely reducing and/or high-temperature conditions. Indeed, terrestrial olivine is Cr-free except for some high-T occurrences from Archaean komatiites, inclusions in diamonds, and ultrabasic pseudotachylytes. Deserpentinization is an important fluid release process in subduction zones. One of the best studied examples of this process occurs in Cerro del Almirez (SE Spain), where the antigorite-out reaction front ($\text{Atg} = \text{Ol} + \text{Opx} + \text{Chl} + \text{H}_2\text{O}$) at eclogite facies conditions is well preserved. Large elongate olivine crystals (similar to spinifex textures in komatiites) at the reaction front contain abundant exsolution lamellae of Cr-magnetite, and estimated primary compositions of the elongate olivine show high Cr content (0.1-0.4 wt% Cr_2O_3), leading to a proposal of the spinifex-like textured peridotite being pseudotachylyte ($> 1600 \text{ }^\circ\text{C}$, Evans & Cowan, 2012), in contrast to the generally held view that the elongate olivine crystallized under ambient subduction-zone T ($\sim 680 \text{ }^\circ\text{C}$ at 1.9 GPa) but high supersaturation conditions.

To better understand the dehydration process of serpentinite in subduction zones, this study focuses on a deserpentinized peridotite from the Eclogite unit of the Sanbagawa belt (SW Japan). It consists of porphyroblastic olivine ($\sim 70 \text{ vol } \%$, $\text{Mg}\# = 0.952 \pm 0.004$, $\text{NiO} = 0.37 \pm 0.04 \text{ wt } \%$), antigorite ($\text{Al}_2\text{O}_3 = 0.3\text{-}0.5 \text{ wt } \%$), brucite, zoned Cr-spinel and Ni sulfides. Olivine porphyroblasts contain inclusions of antigorite, brucite, magnetite and Ni sulfides, suggesting that the olivine-forming reaction $\text{Atg} + \text{Brc} = \text{Ol} + \text{H}_2\text{O}$ took place after serpentinization of a dunitic protolith. Sporadic occurrences of Ni-rich olivine (up to 8.1 wt% NiO) within the olivine porphyroblasts suggest prograde breakdown of Ni-rich sulfides. Zoned Cr-spinel grains are composed of a chromite core, a ferritchromite mantle, and an irregular-shaped overgrowth of Cr-magnetite. The chromite core, being the only primary mineral preserved, shows Cr-rich/Ti-poor compositions [$\text{Cr}/(\text{Cr}+\text{Al}) = 0.74\text{-}0.76$, $\text{TiO}_2 < 0.14 \text{ wt } \%$] indicative of a forearc wedge mantle origin. The Cr-magnetite rim contains inclusions of Cr-rich olivine ($\text{Cr}_2\text{O}_3 = 0.12\text{-}0.70 \text{ wt } \%$, $\text{Mg}\# = 0.950 \pm 0.004$, $\text{NiO} = 0.37 \pm 0.04 \text{ wt } \%$), in addition to Cr-rich antigorite ($\text{Al}_2\text{O}_3 = 0.5\text{-}3.1 \text{ wt } \%$, $\text{Cr}_2\text{O}_3 = 0.3\text{-}3.9 \text{ wt } \%$), diopside and brucite.

Formation of the Cr-rich olivine inclusions can be explained by dehydration of Cr-rich antigorite that developed around Cr-spinel grains. Slow diffusivity of Cr^{3+} compared to the olivine growth rate may have caused disequilibrium Cr incorporation into olivine under low-T conditions just above the $\text{Atg} + \text{Brc}$ breakdown equilibrium ($\sim 460\text{-}500 \text{ }^\circ\text{C}$). Alternatively, a distinct Cr substitution mechanism ($\text{Cr}^{3+} + \text{Fe}^{3+} = \text{Mg} + \text{Si}$) than that proposed for high-T olivine ($\text{Cr}^{2+} = \text{Mg}$ or $2\text{Cr}^{3+} + \text{vacancy} = 3\text{Mg}$) could explain the low-T formation of Cr-rich olivine. In any case, the local uptake of Cr in olivine from the Sanbagawa metaserpentinite does not imply very high-T conditions, and this weakens the main basis of the pseudotachylyte hypothesis for the spinifex-like textured peridotite in Cerro del Almirez. The geological record on the causal link between deserpentinization and deep earthquake nucleation remains elusive.

Keywords: Cr-rich olivine, antigorite, dehydration, subduction zone

振幅—継続時間スケーリングから推測される四国西部における深部低周波微動のスケール長の空間変化
Spatial variation in scale length of deep low-frequency tremor inferred from duration-amplitude scaling in western Shiko

堀野 一樹^{1*}; 平松 良浩²; 水上 知行²; 小原 一成³; 松澤 孝紀⁴

HORINO, Kazuki^{1*}; HIRAMATSU, Yoshihiro²; MIZUKAMI, Tomoyuki²; OBARA, Kazushige³; MATSUZAWA, Takanori⁴

¹ 金沢大学大学院自然科学研究科自然システム学専攻, ² 金沢大学理工研究域自然システム学系, ³ 東京大学地震研究所, ⁴ 防災科学技術研究所

¹Division of Natural System, Graduate School of Natural Science and Technology, Kanazawa University, ²School of Natural System, College of Science and Engineering, Kanazawa University, ³Earthquake Research Institute, University of Tokyo, ⁴National Research Institute for Earth Sciences and Disaster Prevention

Slip properties on plate interface vary largely along dip direction from seismic to aseismic slip. At the transition zone at depths of 25-35 km, non-volcanic deep low-frequency (DLF) tremor and short-term slow slip event occur in the Nankai subduction zone. Recent detailed studies (e.g. Obara, 2010) reveal along dip and along strike variations in the occurrence and the migration of DLF tremor in the transition zone. We report here an along dip variation in scale length of DLF tremor inferred from duration-amplitude scaling in the western Shikoku.

A physical process of natural phenomena is reflected by scaling law, for example, frequency of occurrence versus size distribution. Watanabe et al. (2007) reported that a duration-amplitude distribution of DLF tremor shows a better fit to the exponential model rather than the power-law model, which is different from regular earthquakes. We investigate the duration-amplitude distribution of DLF tremor using Hi-net data in the western Shikoku. The procedure of analysis is the same as that of Watanabe et al. (2007).

We focus on the slope of the exponential distribution for the duration-amplitude distribution of DLF tremor. The value of the slope is small in the western area and large in the eastern area. Noting along dip direction, we can recognize a weak variation of the value of the slope. Deeper DLF tremor tends to show a larger value of the slope than shallower DLF. A large value of the slope means a small scale length and vice versa.

Beneath the western Shikoku, the configuration and the age distribution of the subducting Philippine Sea plate changes significantly along the strike, generating a large variation in a thermal structure. Such a variation causes various modes of serpentinization in the hanging wall mantle. The resultant structures due to the different modes are the most likely cause of the detected transition of the scale length.

キーワード: 深部低周波微動, スケーリング則, 沈み込み帯, 規模別頻度分布, 蛇紋岩化

Keywords: deep low-frequency tremor, scaling law, subduction zone, size distribution, serpentinization